9-1-2022

Optimal Inverter And Wire Selection For Solar Photovoltaic Fencing Applications

Koami Soulemane Hayibo
Western University, khayibo@uwo.ca

Joshua M. Pearce
Western University, joshua.pearce@uwo.ca

Optimal inverter and wire selection for solar photovoltaic small-scale fencing applications

Koami S. Hayibo 1 and Joshua M. Pearce 1,2*
1. Department of Electrical & Computer Engineering, Western University, London ON, Canada
2. Ivey Business School, Western University, London ON, Canada
* Correspondence: joshua.pearce@uwo.

Optimal inverter and wire selection for solar photovoltaic small-scale fencing applications

Koami S. Hayibo 1 and Joshua M. Pearce 1,2*
1. Department of Electrical & Computer Engineering, Western University, London ON, Canada
2. Ivey Business School, Western University, London ON, Canada
* Correspondence: joshua.pearce@uwo.

Abstract

Despite the benefits and the economic advantages of agrivoltaics, capital costs limit deployment velocity. One recent potential solution to this challenge is to radically reduce the cost of racking materials by using existing farm fencing as vertical photovoltaic (PV) racking. This type of fenced-based PV system is inherently electrically challenging because of the relatively long distances between individual modules that are not present in more densely packed conventional solar PV farms. This study provides practical insights for inverter selection and wire sizing optimization for fence-based agrivoltaic systems. Numerical simulation sensitivities on the levelized cost of electricity (LCOE) were performed for 1) distance from the fence to the AC electrical panel, 2) inverter costs, and 3) geographic locations. The results showed that microinverters had better performance when the cross-over fence length was under 30 m or when the system was designed with less than seven solar PV modules, whereas string inverters were a better selection for longer fences. The cross-over number of modules depends significantly on the cost of the inverters, which is a parameter that influences the system's design. The capital costs for a fence retrofit is far less than for any form of conventional PV racking. In addition, the LCOE of the vertical fencing solar agrivoltaic system can be competitive with conventional ground-mounted solar PV for the niche of small-farmers, but further studies are needed for an in-depth cost comparison analysis of the two systems for agrivoltaics and vertical PV fencing systems for large-scale multi-hectare agricultural applications.

Keywords: agrivoltaic; inverter; photovoltaic fencing; vertical photovoltaics

1. Introduction

In order to utilize solar photovoltaic (PV) technology to offset enough fossil fuel production to halt climate destabilization, large surface areas are needed [1]–[6]. Cities, where the majority of humanity calls home [7], lack adequate surface area for PV to meet electrical needs even without including electrification of heating and transportation to eliminate the need for all fossil fuel combustion. Large surface areas are available in rural areas, the center of food production [8]. Such land-use conflicts, once relegated to wind farm development [9]–[12], are increasingly challenging large-scale PV projects as they can interfere with agricultural production [3], [5], [13], [14]. These problems are slated to worsen with the human population increasing by 1.15%/year [15], and thus food production needs to be increased by 70% by midcentury to feed all 9.1 billion people expected to be alive at the time [16]. Historically, the good-intentioned conversion of cropland to ethanol production for fuel increased food costs and aggravated global hunger [17]–[20]. Agrivoltaics, a relatively new technology that co-develops land for both PV and agricultural food production, can meet the goals of both applications, not only without conflict, but also some synergies [21]–[23]. These synergies, which include protection of plants from direct sunlight and overheating, increase sub-panel water retention for plants, and lower operating temperatures for PV, enable agrivoltaics to at least provide the option of increasing global land productivity by 35-73% [21], while minimizing agricultural displacement for energy [22]–[25]. Agrivoltaics is under intense research investigation including aloe vera [26], aquaponics (aquavoltaics) [27], lettuce [28], [29], grapes [30], maize or corn [31], [32], and wheat crops [33]. Agrivoltaic studies,

in general, show either marginal impacts on various crop productions or sometimes an increase, particularly of shade-tolerant leafy vegetables like lettuce, which prefer partial shading from PV [34]. Agrivoltaics creates a mutually beneficial symbiosis [35]–[37]. Socially, it is supported by farmers [38], the PV industry [39], and the general public [40]. Despite these benefits and the economic advantages of agrivoltaics [22], the cost of solar agrivoltaics system, especially for small-scale farmers, remain capital intensive. This is in part due to the capital costs of the balance of system (racking and electrical installations) that represent 32% of the total cost of the system (not including soft costs) [41]. One recent potential solution to this challenge is to radically reduce the cost of racking materials by using existing farm fencing [42] to make agrivoltaic systems. In such systems, PV modules can be mounted with metal cable zip ties to a wide variety of existing fencing and still meet mechanical and civil codes [42]. Such fenced-based PV systems not only create solar electricity that has economic value, but can act as wind barriers [43], [44]. Also, the fences serve as a deterrent against wild animals that can otherwise intrude on the farm and destroy crops or harm the animal husbandry [45], [46].

This type of fenced-based PV system is inherently electrically challenging because of the relatively long distances between individual modules compared to the more densely packed conventional solar PV farms. In addition, the nature of such arrays means that farmers could install such PV systems themselves with existing tools, but are unlikely to be PV system design experts. How should such systems be designed electrically? How to select the best inverter suitable to the fence-based PV application?

This study is designed to answer these questions for small farmers for the first time and provide practical insights for inverter and wire selection for PV system designers and small-scale farmers who want to improve the value of their business. Through numerical simulation studies it will provide the best inverter for solar fences application depending on the length of the fence, with a particular focus on the wire sizing optimization for microinverters and central inverters. Sensitivities are run on 1) distance from the fence to the AC electrical panel, 2) inverter costs, and 3) geographic locations. Using the costs of the components the levelized cost of electricity is compared to conventional PV systems as a whole and balance of systems only.

2. Material and Methods

The methodology used in this study combines electrical cables section calculations and solar PV system design techniques into a practical calculation algorithm that outputs the levelized cost of electricity (LCOE) of a solar PV system installed on a vertical fence used for agricultural purposes. The algorithm is applied to a vertical solar fencing, by considering either a string inverter or microinverters, to determine the appropriate type of inverter that needs to be used for an optimal cost of the system depending on the length of the fence. A base case analysis is conducted followed by a sensitivity analysis of the key parameters.

2.1. Solar agrivoltaics system layout

A recent study [42] has performed a wind load study on solar PV modules installed on different types of farm fences. According to the results, when a single solar PV module is installed between the posts of a fence with posts, the fencing can sustain up to 209 km/h of incoming wind gust. As a result, in this study the geometrical layout considered is that of a fence with posts where the posts are spaced by a 5m-distance as shown in Figure 1 [47]–[49]. A single module is installed in the space between two posts, and the modules are interconnected through either a string inverter or microinverters and then connected to the AC electrical panel that will inject the energy from the modules into the grid. The layout for these systems is shown in Figure 1.

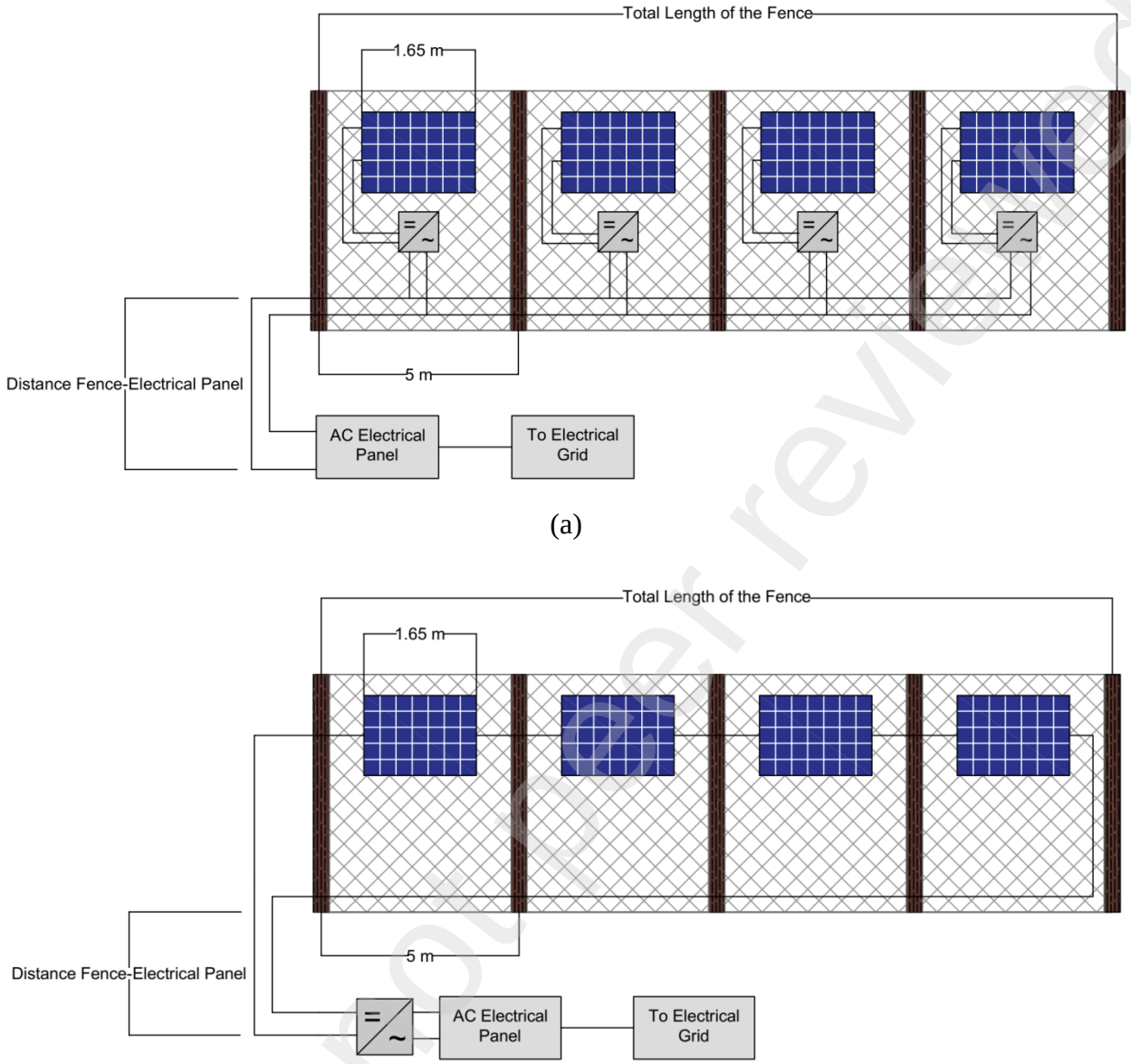

Figure 1. Layout of the fence with the solar PV modules (example of 4 modules). (a) – Microinverter-based system. (b) – String inverter-based system.

2.2. Solar PV system design

The design of the solar PV system is performed using the open-source System Advisor Model (SAM) developed by the National Renewable energy Laboratory (NREL) [50]. The part of the solar PV system that is of interest in this study includes the solar PV modules, the electrical wiring design, and the DC to AC inverters. The AC electrical panel as well as the connection to the grid are out of the scope of the present study. One of the design parameters this study focused on is the type of inverter used to convert the DC power generated by the PV modules into AC power that is fed to the grid. The inverters used in this study have been selected from the SAM software database. The other important parameter is the choice of electrical cables. During the design of an electrical system, cables are a key aspect to ensure

the system will operate as expected under full load conditions and is needed to be selected to ensure that the system will survive electrical faults events [51]. The design choice of a cable in an electrical system depends on several parameters, including the nature of the current flowing in the system (AC or DC), the nominal voltage of the system V_{nom} (V), the nominal current of the system I_{nom} (A), the desired voltage drop ΔV (%), the maximum ampacity rating of the cables I_z (A) provided by the manufacturer as well as the operating temperature of the cables[51]–[53].

2.2.1. Microinverter-based PV system

In the case of a microinverter (mi)-based solar fencing system, each PV module is connected to a single microinverter and the microinverters are connected in parallel. As a result, the overall DC voltage input $V_{DC_{mi}}$ (V) of each microinverter is equal to the maximum power point voltage V_{mpp} (V) of the module it is connected to.

$$V_{DC_{mi}} = V_{mpp} \quad (1)$$

The AC outputs of the microinverters are connected in parallel, therefore the overall output voltage of the AC side of the system $V_{AC_{syst}}$ (V) is the same as the rated output voltage of a single inverter $V_{AC_{mi}}$ (V).

$$V_{AC_{system(mi)}} = V_{AC_{mi}} \quad (2)$$

On the other hand, the maximum current in the AC part of the system $I_{AC_{mi}}$ (A) is obtained by dividing the rated AC power $P_{AC_{mi}}$ (W) of the inverter by the system AC voltage.

$$I_{AC_{mi}} = P_{AC_{mi}}/V_{AC_{mi}} \quad (3)$$

The value of the system's AC voltage and the AC current are used to design the AC cables running from the furthest module's microinverter to the AC electrical. The cables are designed to have a maximum AC loss of 1%. The section of the AC cable is calculated by Equation (4):

$$S_{AC_{mi}} = b \times \frac{\rho \times L_{mi} \times I_{AC}}{\Delta V \times V_{AC_{system(mi)}}} \quad (\text{mm}^2) \quad (4)$$

Where ρ (Ω/mm^2) is the resistivity of the cable adjusted to the temperature, L_{mi} (m) is the length from the last module to the AC electrical panel (See Figure 1a), and b is a coefficient that equals 2 for the single-phase AC cables [52]. After the section of the cable is determined, the chosen commercial cable's gauge is used to calculate the actual voltage drop that corresponds to the actual AC wire losses. The fact that the microinverters deliver power at a power factor of 1 [54], combined with the fact that the study is considered in steady state application explains the reason why the cable reactance is not included in this study [52].

The calculated AC losses are then used as input to SAM for simulation of the systems. In the case of the microinverter, the DC losses are set to zero because the modules are directly connected to the microinverters through their native cables that are designed to minimize the DC losses. Furthermore, the mismatch losses are set to zero as well because using individual inverters for each module ensures that

variation in the production of a module will not affect the production of other modules [55], [56]. The microinverter that was used in the simulation is the Enphase IQ7 [54].

2.2.2. String inverter-based PV system

The design of the system using the string inverter (si) begins by the choice of an inverter that can support the string voltage of the series-connected PV modules. Here, the modules are connected in a series string in the DC part of the system and a DC cable is used to connect the string to the inverter. The inverter is assumed to be located near the AC electrical panel. The DC voltage of the system is the product of the total number of modules N and the maximum point voltage of a single module V_{mpp} (V).

$$V_{DC_{si}} = V_{mpp} \times N \quad (5)$$

The maximum current that can circulate in the DC part is the same as the maximum current of a single module. The current that was considered in this study is the short-circuit current I_{SC} (A) of the modules to ensure that fault cases are covered.

$$I_{DC_{si}} = I_{sc} \quad (6)$$

The DC cables are also designed to have a maximum loss of 1%. The section of the DC cable is calculated by Equation (7):

$$S_{DC_{si}} = \frac{\rho \times L_{si} \times I_{sc}}{\Delta V \times V_{DC_{si}}} \quad (\text{mm}^2) \quad (7)$$

Where ρ (Ω/mm²) is the resistivity of the cable adjusted to the temperature, and L_{si} (m) is the combined length of the positive pole cable and negative pole cable. In this study, the type of cable that have been analyzed are made of copper wires, and the cable length is calculated as shown on Figure 1b. After the section of the cable is determine, the chosen commercial cable's ampacity is compared to the maximum current that can flow through the system to ensure the cable will be able to sustain fault current. Then, the actual voltage drop is determined that corresponds to the actual DC wire losses.

The real DC losses are used as input to the SAM simulation. Also, because of the proximity of the inverter to the AC electrical panel, the AC losses are considered to be zero. The mismatch losses are considered here because the losses in a single PV module will be affecting the output of the other modules since the modules are connected in series.

2.3. Common design aspects of the two systems

Apart from the choice of the inverter and the cables, the design specifications are the same for both the microinverter-based system sand the string inverter-based system. The location chosen for the study is the county of Baraga located in the state of Michigan in the United States. The PV module used for the simulation is the Trina Solar TSM-230 [57]. The TSM-230 solar module has a length of 1.65m and a width of 0.992m, and these dimensions comply with the wind load calculation performed by Sudha et al. [42] using a module of area 2m by 1m**.** In this study, shading calculations were not included as it was considered that the fences were clear from any nearby obstacles. Also, one advantage of installing solar

PV modules vertically on a fence is that there is no mutual shading form one module onto the others. The solar PV modules are installed with an azimuth of 180°, or south facing, since the county of Baraga is in the northern hemisphere. The tilt angle is set to 90° in SAM. The two systems are connected to the grid through the AC electrical panel and are grid-interactive, no local loads are connected to the system. Therefore, the electric load has been set to zero in SAM to account for the absence of local loads in the system.

The simulation is centered around the incremental analysis of the system design and energy production based on the fence length or number of modules that are installed along the fence. The total number of simulations is set to 15, which is determined by the maximum number of microinverters that can be interconnected [54]. An open source script [58]has been written in SAM lk scripting language [59] to automate the simulation for both systems. The cost calculations have been included in the scripts. The script handles for each inverter, the calculation of the theoretical cable section using Equation (1) through Equation (7) as well as the choice of the commercial cable and the price per meter of the cable. Then, the real line losses are calculated. After that the SAM parameters are set using the values shown in Table 1. The script is run in a loop for different number of modules (1 to 15), and the lifetime energy output of the system is captured and used in the calculation of the LCOE at each iteration of the loop.

Table 1. Value of the technical parameters used in the base case simulation.

Parameter	**Microinverter-based System**	**String Inverter-based System**
Location	Michigan	
Inclination (°)	90	
Azimuth (°)	180	
Module annual degradation rate (%)	0.5 [60], [61]	
AC wiring losses (%)	Calculated	0
DC wiring losses (%)	0	Calculated
Mismatch losses (%)	0	2 [62]
Lifetime of the system (years)	25 [57]	
Lifetime of the string inverter (years)	-	15 [63], [64]
Lifetime of the microinverter (years)	25 [54], [55]	-

The detailed algorithm used in the simulation script is shown on the flowchart in Figure 2.

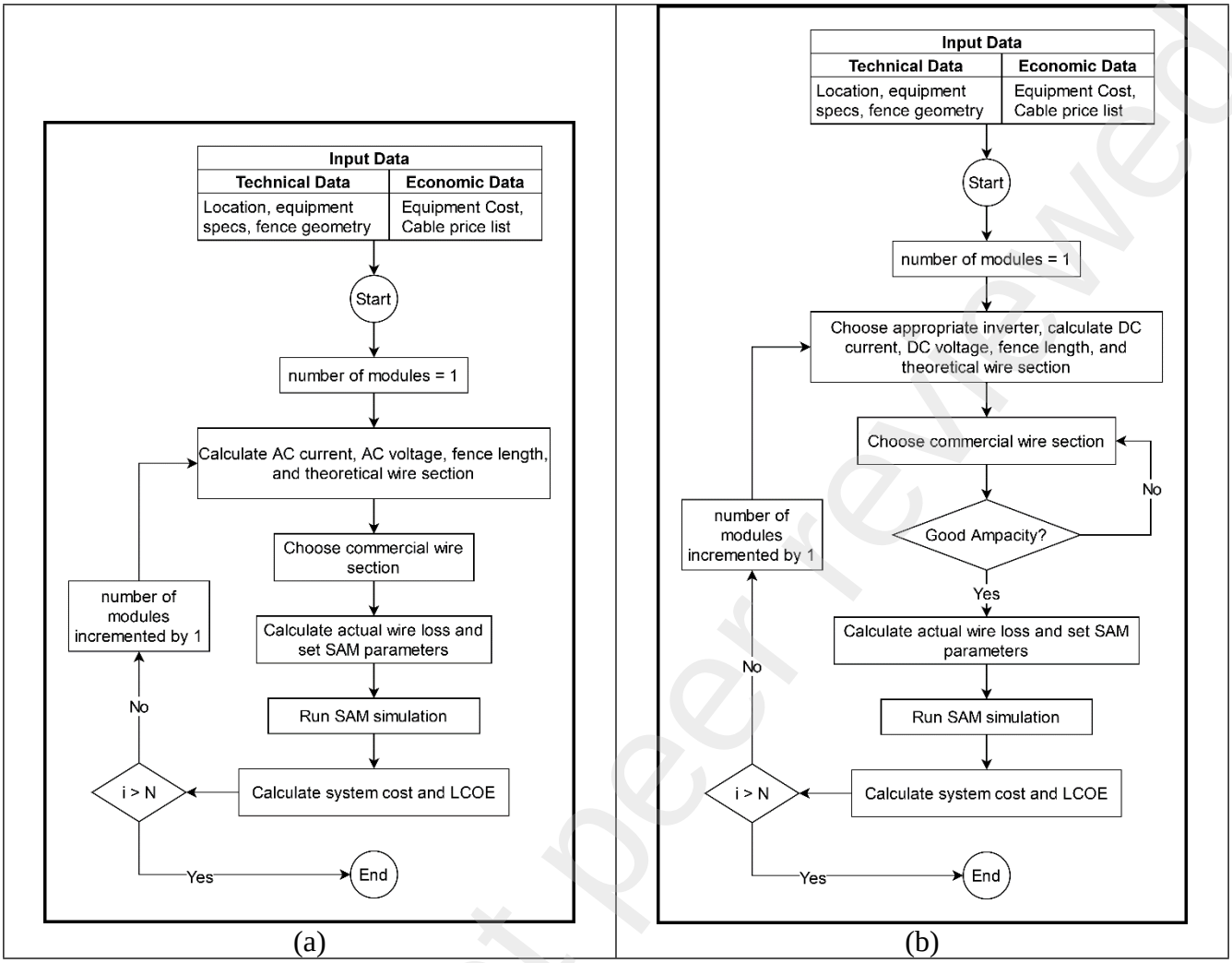

Figure 2. Algorithms developed for the calculation of the LCOE of the two systems using SAM scripting language lk. (a) – Microinverter system algorithm. (b) – String inverter system algorithm.

2.4. LCOE calculation

To compare the performance of the two systems, a levelized cost of electricity method has been used. A complete levelized cost of electricity LCOE (USD/kWh) calculation usually accounts for the cost of all components of the energy generating systems, in this case the solar modules C_{PV} (USD), the inverters C_{inv} (USD), the balance of system (including cabling and racking cost), labor costs C_{labor} (USD), installers overhead costs C_{over} (USD), land costs C_{land} (USD), as well as sales taxes C_{tax} (USD). The calculation of the levelized cost of electricity also factors in the energy generated throughout the lifetime of the system [60], [65]–[67]. The complete levelized cost of electricity is calculated as follows:

$$LCOE = \frac{C_{PV} + C_{inv} + C_{cables} + C_{bos} + C_{labor} + C_{over} + C_{land} + C_{tax}}{\sum_{0}^{i} (E \times F)} \quad (USD/kWh) \qquad (8)$$

In Equation (8), the balance of system cost has been split into C_{cables} that is the cost of cables, and C_{bos} that is the cost of the balance of system not including the cables. E (kWh) is the yearly energy produced by the PV systems considering the annual degradation rate of the modules (0.5% per year), F (%) is the discount factor, and i is the number of years considered for the study which is equal to the guaranteed lifetime of the modules.

For the purposes of this study the LCOE is restricted to the cost of the modules, the cost of the inverter, the cost of the cables, and the cost of the structural balance of systems, which in this case represent the zip-ties that will be used to install the modules on the fence. This is because the cost of the inverter and the cost of the cables are parameters that depends on the system design, while the rest of the parameters remain the same for the two systems (Equation (9)). Also, the discount factor is a parameter set by the utilities [60], therefore it is not included in the calculation of the LCOE.

$$LCOE = \frac{C_{PV} + C_{inv} + C_{cables} + C_{bos}}{\sum_{0}^{i} E} \qquad (USD/kWh) \quad (9)$$

The lifetime of the system considered in this study is $i = 25$ years aligning with the linear power warranty offered by the module manufacturer [57]. Microinverters are known to have a longer operational lifetime than string inverter. Microinverters currently have a lifetime of 25 years backed up by the product warranty offered by the manufacturers [54], [55]. As a result, the microinverters do not need replacement during the lifetime of the PV system. On the other hand, the average lifetime of string inverters has been estimated in past studies to be less than 15 years [63], [64]. Hence, in the string inverter-based solar fence PV system, the inverter is replaced once during the lifetime of the system.

The cost of the PV modules and the cost of the two types of inverters are obtained from the NREL report on PV systems cost benchmark [41]. The modules cost per Wdc in the case of small PV installers is 0.61 USD/Wdc while the cost of the inverters for the same category of installers are 0.29 USD/Wdc and 0.14 USD/Wdc for the microinverters and the string inverters, respectively [41]. The cost of the string inverter has been given per inverter and is doubled in this study to account for the shorter lifetime of the string inverter. The costs of both the AC and DC cables are obtained for each type of cable gauges ranging from 0.5 mm² to 120 mm² by averaging the pricing list cost of two major cable manufacturers [68], [69]. The simulation parameters for both systems are shown in Table 2.

Table 2. Value of the economical parameters used in the base case simulation.

Parameter	**Microinvcerter-based System**	**String Inverter-based System**
Cost of PV modules (USD/kWdc)	0.61 [41]	
Cost of string inverter (USD/kWdc)	-	0.14 [41]
Cost of microinverter (USD/kWdc)	0.29 [41]	-
Cost of the cables	Average from price list from two cable manufacturers [58], [68], [69]	
Cost of zip-ties (USD/module)	7.8 [70]	

3. Sensitivity Analysis

Some of the parameters that are used in the current study have a location-based or time-based value. To understand the robustness of the system design algorithm and the consequent choice of the type of inverter, a sensitivity analysis has been conducted on the following parameters: 1) the distance from the fence to the AC electrical panel, 2) the cost of the microinverter, 3) the cost of string inverter, and 4) the geographical location of the system. In the sensitivity analysis, the effect of the fluctuation of each of the parameters on the results has been analyzed by varying the parameter of interest while the other parameters are maintained at the value used in the base case. For each instance of the parameter the sensitivity analysis is performed on, the algorithms in Figure 2 are run for each inverter.

Table 3 shows the values used during the sensitivity analysis for the distance from the fence to the AC electrical panel, the cost of the microinverter, and the cost of the string inverter.

Table 3. Value range of the parameters used for the sensitivity analysis

Parameter	**Low Value**	**High Value**	**Increment**	**Source**
Distance from the closer end of the fence to the AC electrical panel (m)	20	160	10	This study
Cost of microinverter (USD/kWdc)	0.14	0.44	±0.05	NREL [41]
Cost of string inverter (USD/kWdc)	0.04	0.29	±0.05	NREL [41]

For the geographical location sensitivity analysis, four different locations have been considered in the southern hemisphere, seven distinct locations are analyzed in the northern hemisphere, and one location close to the equator is investigated. These locations have been chosen to cover approximately every 10-latitude degree where there is human population concentration and available solar irradiation as shown in Table 4. The azimuth for the locations situated in the northern hemisphere, was set to the 180° (south-facing) while the azimuth was set to 0° (north-facing) for the locations situated in the southern hemisphere. Additionally, for the location closest to the equator (Libreville), an additional sensitivity analysis is run on the azimuth to determine the orientation that yields the lowest LCOE.

Table 4. List of the locations included in the sensitivity analysis

Location	**Latitude (°)**	**Country**
Helsinki	59.97	Finland
Winnipeg	48.89	Manitoba - Canada
L'Anse	46.77	Michigan - United States
Madrid	40.41	Spain
Cairo	30.05	Egypt
Mexico City	19.45	Mexico
Conakry	9.53	Guinea
Libreville	0.4	Gabon
Dar es Salaam	-6.83	Tanzania
Brasilia	-15.79	Brazil
Johannesburg	-26.19	South Africa
Melbourne	-37.83	Australia

4. Results

4.1. Base case results

The results of the base case simulation are displayed in Table 5. The values of the lifetime energy (kWh), the chosen cable section (mm²), the system cost (USD), as well as the LCOE (USD/kWh) are shown for the microinverter-based system and the string inverter-based system. The lifetime energy production shows that the microinverter system has a higher energy output than the string inverter-based system. For example, for a single module, the microinverter-based system has a lifetime output of 5.1 MWh while the string-based inverter has a lifetime output of 5 MWh. And when the number of modules is set to 15 (maximum number of microinverters that can be connected in parallel), the microinverter-based system has a lifetime energy generation of 76.7 MWh while the string inverter-based system has a lifetime production of 73.7 MWh. On the other hand, the cost of the microinverter system has a higher increase rate as compared to the cost of string inverter-based system. For a single module, the microinverter-based system has a total cost of 216 USD, and the string inverter-based system has a cost of 379 USD; while for 15 modules the total costs are 4,884 USD and 3,415 USD for the microinverter-based system and the string inverter-based system, respectively. As a result, the LCOE of the microinverter-based system rises with the increases of the number of modules while the LCOE of the string inverter-based system decreases with an increase in the number of modules as shown on Figure 3.

Table 5. Results of the base case simulation for the microinverter-based system and the string inverter-based system

		Microinverter				String Inverter			
Fence Length (m)	**Modules Quantity**	**Lifetime Energy (kWh)**	**Cable Section (mm²)**	**System Cost (USD)**	**LCOE (USD/kWh)**	**Lifetime Energy (kWh)**	**Cable Section (mm²)**	**System Cost (USD)**	**LCOE (USD/kWh)**
5	1	5,115	0.5	216	0.042	5,000	35	379	0.076
10	2	10,210	1.0	446	0.044	9,635	25	576	0.060
15	3	15,357	2.5	687	0.045	14,687	25	758	0.052
20	4	20,480	4.0	935	0.046	19,608	16	985	0.050
25	5	25,525	4.0	1,160	0.045	23,531	16	1,217	0.052
30	6	30,660	6.0	1,426	0.047	29,514	10	1,389	0.047
35	7	35,840	10.0	1,763	0.049	34,459	10	1,614	0.047
40	8	40,888	10.0	2,004	0.049	37,469	10	1,839	0.049
45	9	46,091	16.0	2,448	0.053	44,655	10	2,064	0.046
50	10	51,144	16.0	2,706	0.053	46,905	10	2,289	0.049
55	11	56,176	16.0	2,963	0.053	54,735	10	2,514	0.046
60	12	61,428	25.0	3,579	0.058	59,670	10	2,740	0.046
65	13	66,475	25.0	3,861	0.058	64,884	10	2,965	0.046
70	14	71,504	25.0	4,143	0.058	69,811	10	3,190	0.046
75	15	76,747	35.0	4,884	0.064	73,712	10	3,415	0.046

On, Figure 3, the LCOE (USD/kWh); that includes for each system the cost of the modules, the cost of the inverter, and the cost of the cables; is studied for different values of the fence length. Here, the fence length has a direct equivalence with the number of modules in the system. A single module is installed in the space between two posts of the fence, therefore there is one module for each 5m of fence.

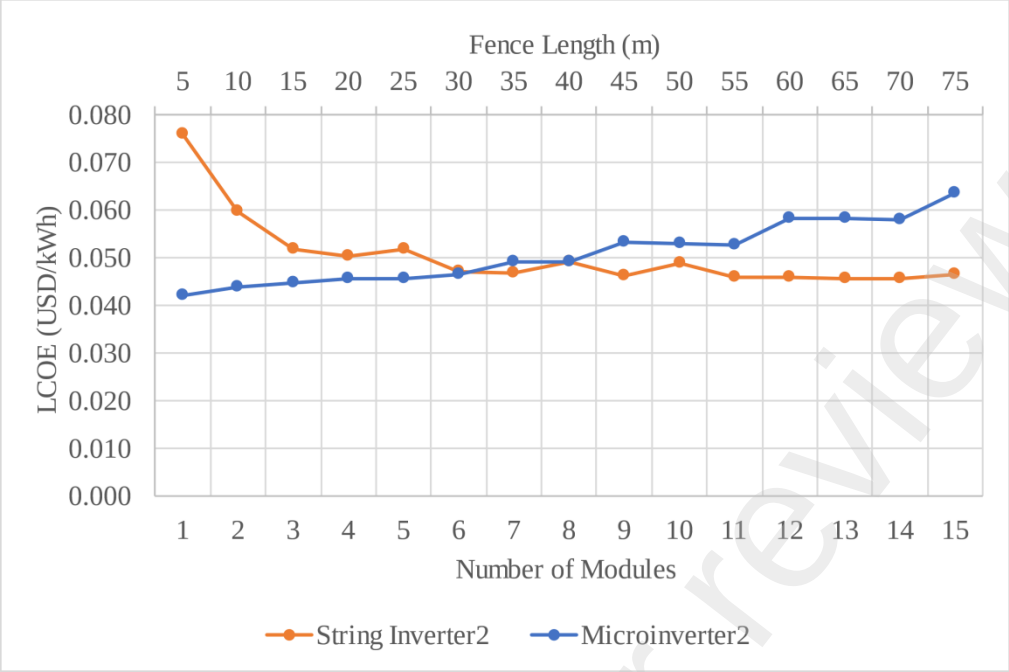

Figure 3. Comparative LCOE cost of the system (modules, inverter, and cables) depending on the length of the fence for the microinverter-based systems and the string inverter-based system.

The minimum value of the LCOE for the microinverter case is 0.04 USD/kWh for a single module or a fence length of 5m, and the maximum value for the same type of inverter is 0.06 USD/kWh for 15 modules or a fence length of 75m. From Figure 3, the curve of the LCOE for the microinverter increases with the number of modules installed in the system. On the other hand, the value of the LCOE for the string inverter- based system varies from 0.07 USD/kWh for a fence length of 5m or a single module to 0.04 USD/kWh for a fence length of 75m or 15 modules (the limit on the number of parallel connections possible with the microinverter) [54]. The LCOE for the string inverter-based system decreases when the number of modules increases. The plot of the LCOE for each of the two types of system crosses at a fence length of 30m or 6 modules, showing that the LCOE for the string inverter-based system is higher than the LCOE of the micro-inverter-based system when the length of the fence is lower than 30m. When the number of modules is greater than 6 modules, then the LCOE for the string inverter is lower than that of the microinverter. The trend of the LCOE of the two types of systems observed in Figure 3 is linked to the choice of the cables that are used respectively in the two systems as shown on Figure 4.

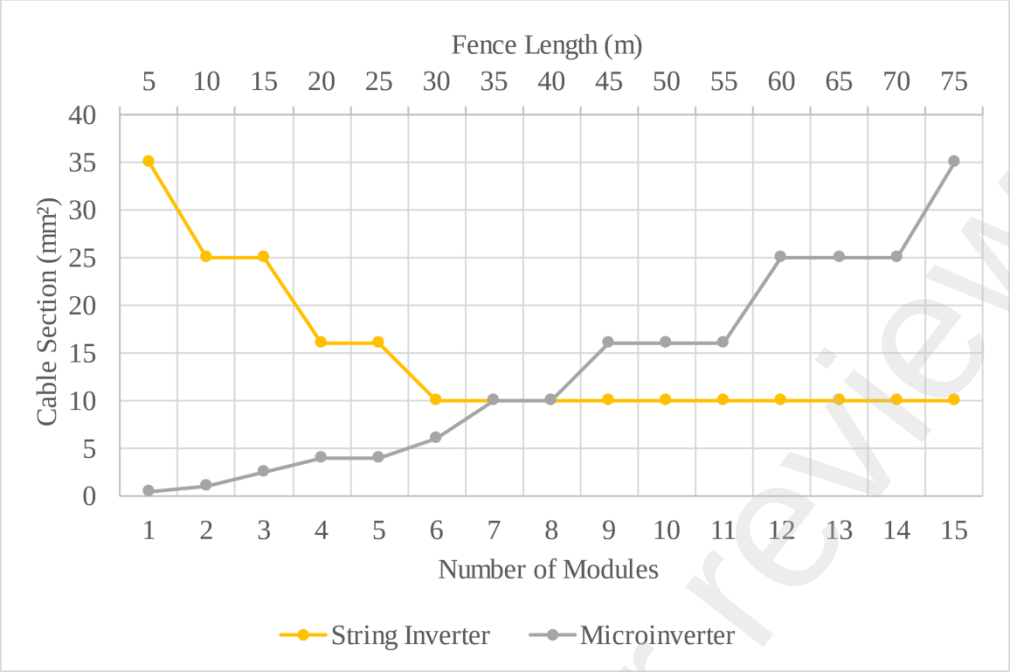

Figure 4. Comparison of the sections chosen for the cable at each simulation step (number of modules from 1 to 15 in an increment of 1)

4.2. Sensitivity results

The sensitivity results are obtained by plotting the cross-over fence length or the fence length at which the LCOE of the two systems cross each other. The cross-over fence length is recorded for different values of the sensitivity parameter.

4.2.1 Distance from the fence to the AC electrical panel

In the case of the distance from the fence to the AC electrical panel, the cross-over fence length varies between 30m (6 PV modules) and 25m (5 PV modules) as can be seen in Figure 5. For a distance from the fence to the AC electrical panel between 20m and 60 m, as well as for a distance between 100 and 110m, the cross-over fence length is 30m. On the other hand, this distance is reduced to 25m when the distance from the fence to the AC electrical panel is between 70 and 90 or for distances above 110m. As can be seen from Figure 5, the distance to the fence has only a minor impact on the optimal design.

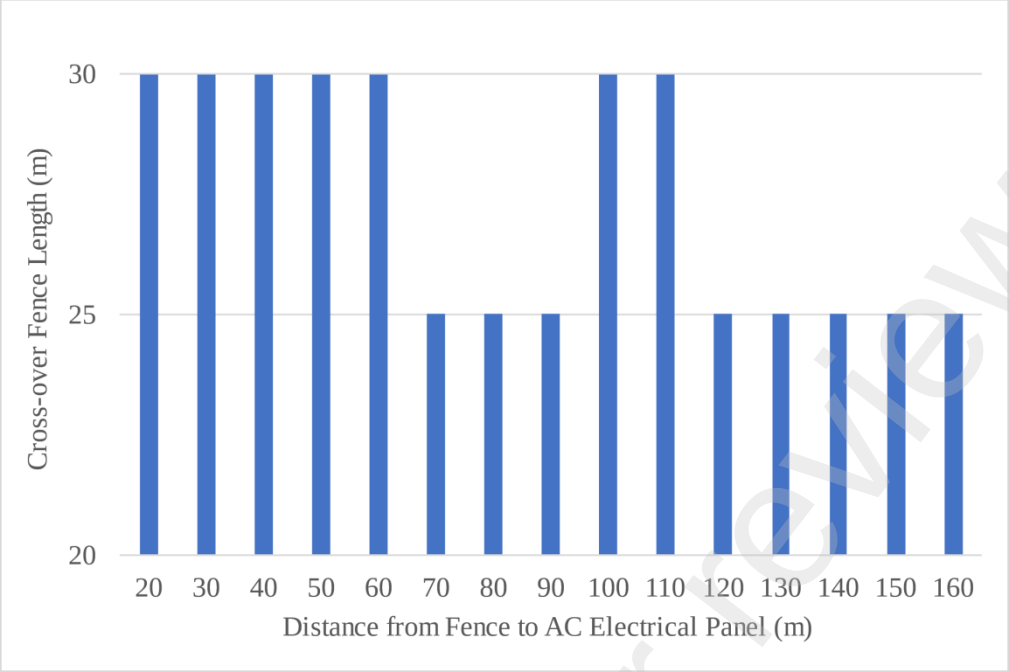

Figure 5. Sensitivity results of the cross-over fence length for different values of the distance from the fence to the AC electrical panel.

4.2.2 Inverter costs

Figure 6 shows the results of the sensitivity analysis when there is a change in the cost of the inverters. The results on Figure 6a clearly show that when the cost of the microinverter goes down while the cost of the string inverter remains unchanged, then the cross-over fence length is increased Similarly, Figure 6b shows that when the cost of the microinverter is maintained at a constant value while the cost of the string inverter is changed, the cross-over fence length decreases with the decrease of the string inverter cost and when the cost of the string inverter is increased, the fence length increases accordingly.

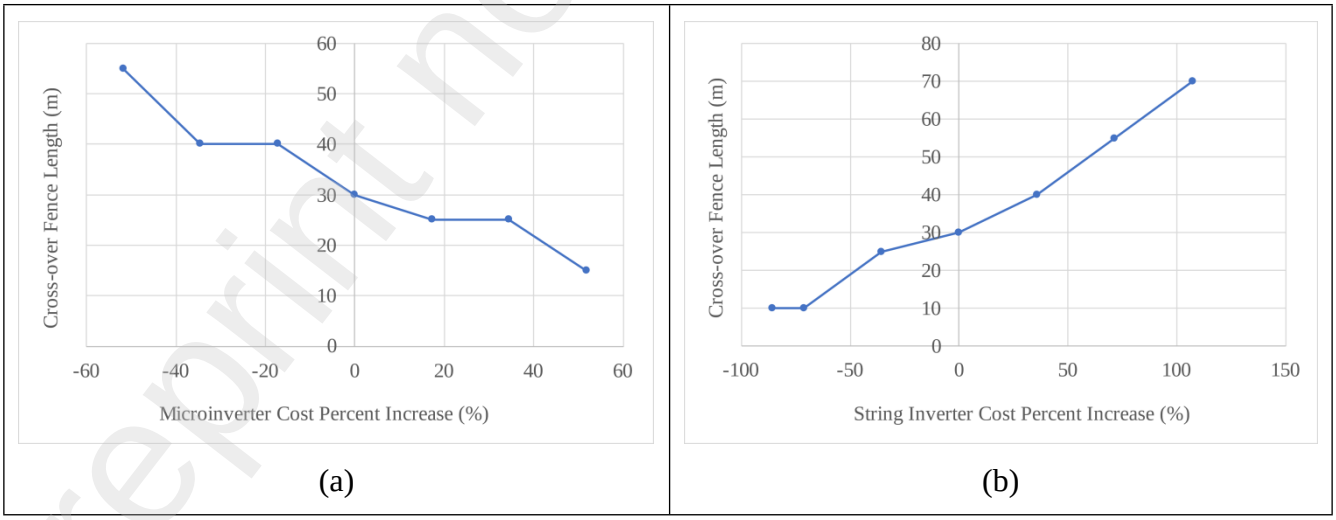

Figure 6. Sensitivity results of the cross-over fence length for a variation of the inverter's cost. (a) Case of the microinverter-based system. (b) Case of string inverter-based system.

4.2.3 Location

Running the simulation for different locations across the world does not impact the cross-over fence length, which remains the same as in the base case (30m or 6 PV modules). Nevertheless, comparing the LCOE at the cross-over fence length for the location results show that the LCOE depends on the location as shown in Figure 7. The highest LCOE for the locations considered in this study is registered for Libreville (0.09 USD/kWh), while the lowest LCOE is obtained for Johannesburg, Winnipeg, Madrid, and Cairo (0.04 USD/kWh). It can be noticed that the LCOE is the highest for the location nearest to the equator. Therefore, an additional sensitivity is run for the case of Libreville, which investigates the orientation of the fence.

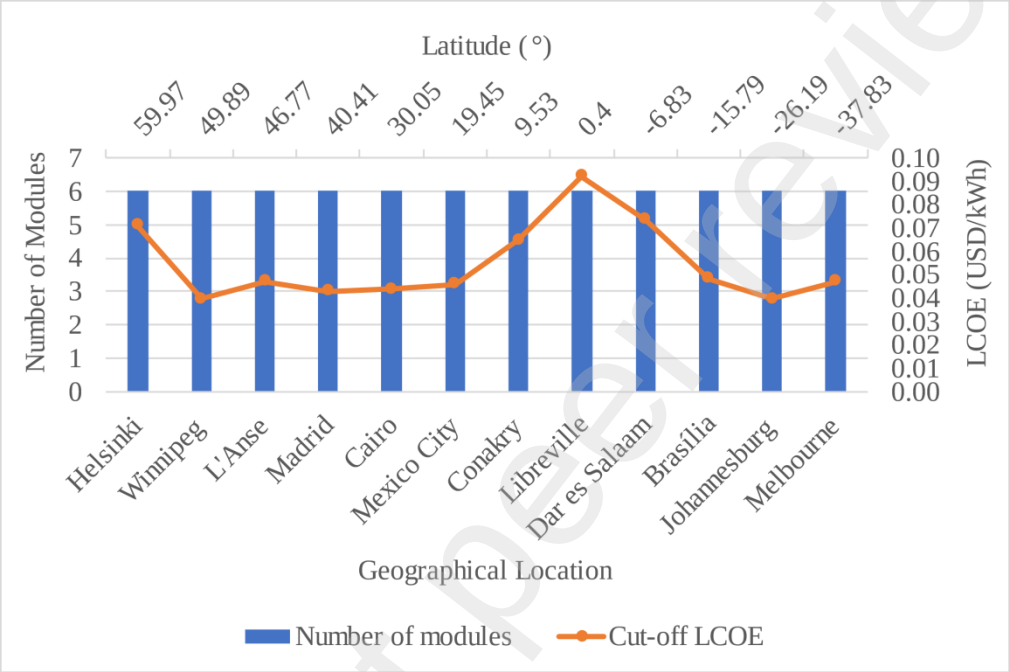

Figure 7. Sensitivity results of the cross-over fence length and the corresponding LCOE for different geographical locations.

Figure 8 shows the results for the specific case of Libreville (near the equator) where several azimuths are analyzed to determine which orientation of the fence yields the lowest LCOE. According to the results, an azimuth of 0° and 180° or north and south orientation yields the highest LCOE (0.09 USD/kWh). On the other hand, and azimuth of 270° or a west-facing orientation yields the lowest LCOE (0.06 USD/kWh).

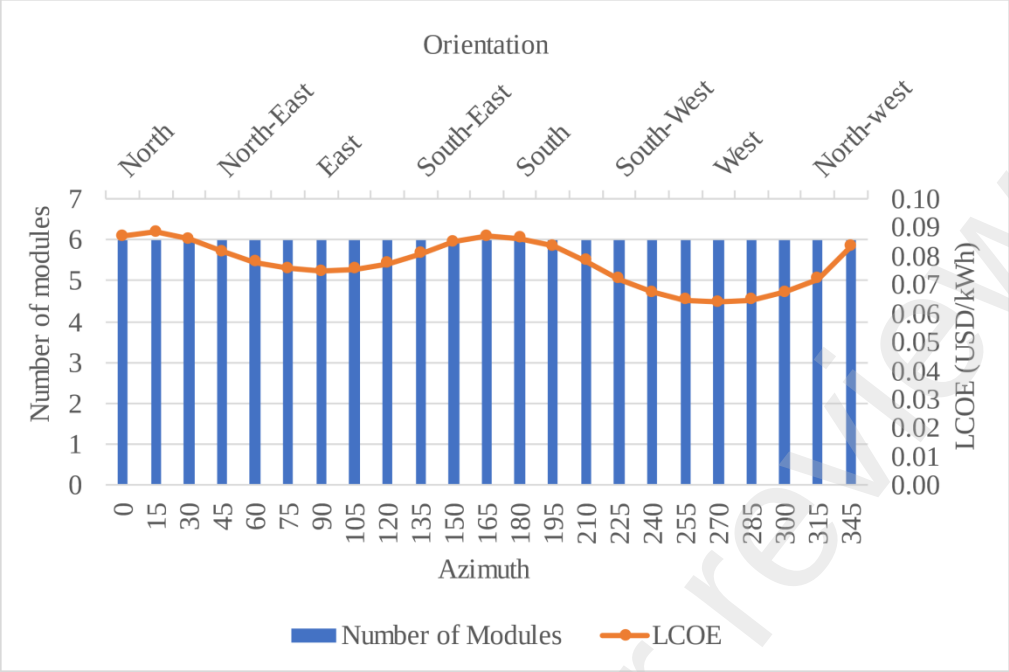

Figure 8. Results of the sensitivity analysis on the orientation (azimuth) of the fence for the case of a location near the equator.

5. Discussion

The base case simulation performed in this study has shown that the LCOE of a solar PV system installed on an existing vertical fence depends on the type of inverter used to convert the DC power into AC power. For the microinverter-based systems, the value of LCOE decreases with an increase in the number of PV modules. Moreover, for the string inverter-based system, the opposite tendency is observed. This observation shows that microinverters are better suited for small-scale vertical solar PV systems installed on fences when the number of modules is less than or equal to 6 with a corresponding LCOE of 0.05 USD/kWh (the LCOE includes all non-labor components of the retrofit: PV, inverter, cables and zip ties). When the number of modules is higher than six or the fence length exceeds 30m, string inverters yield a lower LCOE, as displayed in Figure 4. Figure 4 shows how the cable section varies with the increase in the number of modules, or the fence length, in each case. For the microinverter-based systems, the total current transported in the AC part increases with the number of modules while the voltage remains constant. Therefore, the size of the cables needs to increase to keep the wire losses below 1%. On the other hand, the string inverter-based system uses cables with decreasing sections while the number of modules increases. This information agrees with the increase in voltage in the string inverters as the number of modules increases while the current remains constant in the module string.

According to the sensitivity analysis results, the maximum number of modules under which the microinverter-based system has a lower LCOE than the string inverter-based system (cross-over number of modules) decreases from 6 to 5 when the distance between the fence and the electrical panel is above 60m. This decrease is the result of the increase of the wiring losses in the microinverter-based system. The choice of a higher cable cross-section, which translates into a higher system cost or LCOE, compensates for the increasing wiring losses. For a fence length between 100m and 110m, the cross-over number of modules goes up to six. The increase of the cross-over number of modules results from the difference between the LCOE being in a tenth of cents for these two distances, suggesting that using a string inverter or a microinverter for these specific fence lengths will cause no significant differences in

the LCOE. Additionally, the sensitivity analysis highlights the impact of a change in the inverters' costs on the base case results. If the string inverter cost remains unchanged while the microinverter cost decreases by 52%, the cross-over number of modules will increase from the base case value (6 modules) to 11 modules. On the other hand, if the microinverter cost remains fixed while the string inverter cost decreases by 86%, then the cross-over number of modules will decrease to 2 modules. As a result, the costs of the inverters are clearly the most critical parameter to consider when choosing a type of inverter during the designing of a vertical solar agrivoltaic fence system. Furthermore, the sensitivity results emphasize that the location does not affect the cross-over number of modules. Nevertheless, one crucial observation during the location sensitivity analysis is that the cross-over LCOE varies from one location to another even though the number of modules or the DC power rating of the system is the same across locations. This result reveals that if the value of solar PV equipment is the same across locations, the economic value of solar agrivoltaic fencing depends on the installation site. Installations sites located at higher latitudes in both the northern and southern hemispheres generally have the best LCOE because the tilt of the solar modules (90°) is closer to the latitudes of the locations [71], [72]. When the location is at high latitudes with freezing weather, however, then the LCOE is reduced because the global solar irradiation becomes lower. Further analysis into the location nearest to the equator has shown that an azimuth of 270° (west-facing orientation) will minimize the LCOE. For a location on the equator, an azimuth of 90° (east-facing) or 270º (west-facing) will theoretically yield the maximum energy production or lowest LCOE. In this simulation, the azimuth of 270° has a lower LCOE because SAM algorithm uses the reduced form of solar angle of incidence equation [62], [73]. In the reduced equation of the angle of incidence the difference between the solar azimuth and the surface azimuth is used instead of just the surface azimuth. This introduces a shift in the angle of incidence value that impacts the subsequent variables that are calculated using the angle of incidence. As a result, the incident beam irradiation value is affected as well as the lifetime energy production and the LCOE and can be investigated in more detail in future work.

This study is the first to cover the detailed electrical design of vertical agrivoltaic solar fencing used as an energy generation device; past studies focused primarily on using solar power to energize electrical fences [74]–[77]. The design process developed in the study is aimed at small farmers across the world to bring added value to the existing farming activities and existing fencing infrastructure. The algorithm; and the SAM script for the choice of the inverter and the appropriate cable section are open source [58]. As a result, any small-scale farmer who has access to the open-source SAM software can design and install a solar PV system on an existing farm fence structure. Small-scale farms or farms with a total exploitable area smaller than 20,000 m² are 570 million worldwide, representing 12% of the world's total agricultural land [78], [79]. Most of these small farmland sites are in rural areas where energy costs are extremely high due to the distance and losses of the transmission and distribution lines, and some do not have access to grid electricity. Therefore, solar agrivoltaic fencing applications appear as an attractive alternative to reduce the cost of electricity for small-scale farmers. The reduction of the balance of system cost emphasizes the importance of considering vertical fencing solar agrivoltaic. In the vertical solar agrivoltaic system layout design proposed by Sudha et al. [42], the balance of system cost is reduced to the cost of zip-ties because there is no need for a foundation as in most ground-mounted solar PV systems. Here, existing fence structures replace the foundations. Even though the overall energy production of the vertical fence solar agrivoltaic system is smaller than the energy produced by the optimized ground-mounted solar PV systems, the vertical fence agrivoltaic systems has the potential to compete with land-based systems in terms of LCOE. According to the NREL, the LCOE of conventional residential PV ranges between 0.10 USD/kWh and 0.14 USD/kWh [41]. The different values of LCOE in this study ranged from 0.04 USD/kWh to 0.08 USD/kWh, not including administrative costs, sales costs, installation costs, or taxes. Because the system proposed in this study is a do-it-yourself (DIY) PV system [80], most of the costs listed above do not intervene in calculating the final LCOE cost. Therefore, it is

clear that vertical fencing solar agrivoltaic systems not only have lower capital costs than conventional ground mounted systems, but can also be expected to have a competitive LCOE compared to optimized ground-mounted systems. For example, the LCOE of a microinverter-based fence agrivoltaic system using 6 modules is 0.06 USD/kWh, while the LCOE of an optimized tilted ground-mounted PV system is 0.05 USD. The calculation of these two LCOE is performed in SAM (not including financing and taxes) using the output of the base case simulation and considering the same system parameters for the fence-based system and the optimized ground-mounted system. The substantially lower capital cost giving a similar LCOE is especially compelling for the niche market of small-scale farmers often lacking in capital if the inverter choice and the cable section are optimized. It should also be pointed out that these LCOE values did not include any ancillary benefits that the PV additions to fencing might provide the farmer. It is well established that windbreaks, would be expected to reduce soil erosion [81], [82], may also increase crop quality and crop yield [83]–[85] and may improve water-use efficiency [44] and rebuild soil carbon [86]. These benefits might also occur with the addition of a solar fence acting as a windbreak. Future work is needed to quantify these benefits with modeling and experimental studies.

The results of this study have shown that vertical solar agrivoltaic fences represent a promising niche market research field to lower the solar PV system cost for small-scale farmers. In conventional solar PV systems, the environmental impact of the racking represents 8 to 23% of the total emissions of the system [87], [88]. In the proposed system design, the zip-ties and the existing fences constitute the racking; therefore, although it can be hypothesized that such systems will have an even lower environmental impact than conventional systems, future works is needed to analyze the emissions reductions and overall ecological footprint of the fencing PV system compared to conventional solar PV systems. A complete life cycle analysis needs to be performed on vertical solar agrivoltaic systems to evaluate how much they can contribute to the global climate change mitigation effort. The current study has focused on grid-connected systems. There is, however, no electrical grid access in some locations where small farms are situated [89]. Therefore, future work is needed to analyze a stand-alone vertical fence agrivoltaic system with a backup solution. Future studies can focus on analyzing the battery bank capacity or a combined solar PV-biodiesel generator renewable solution needed in different remote locations to allow an autonomous operation of the vertical agrivoltaic fence system. As this study has focused on small-scale farmers, the logical next topic to investigate is the design of vertical solar fencing for large-scale farms. The complexity of using the proposed system design in large-scale farms increases with the longer distances and the different orientations of each side of the fence. Future studies need to analyze the impact of the distances and the difference in orientation to determine the best layout that will reduce the cost of the system in the case of large-scale agrivoltaic fencing systems. In addition, future work is necessary to investigate using PV modules in place of the fencing itself as well as the potential for having 2, 3, or more modules arranged in vertical rack fencing.

6. Conclusions

This study has performed optimization analysis on the electrical design of a solar agrivoltaic fencing retrofit systems for small-scale farms. The design optimization focused on the electrical components: the inverter selection and the cable cross-section. The analysis compared the energy performance and the levelized cost of electricity of two different systems operating with a microinverter and a string inverter based on the length of the farm fence. The microinverter had better performance when the cross-over fence length was under 30 m or when the system was designed with less than 7 solar PV modules. Above 30 m, or when the installed PV system contains 7 modules or more, using string inverter yields a lower LCOE. An open-source code was developed and made available for farmers to design and build the system with little assistance. The cross-over number of modules depends significantly on the cost of the

inverters, which is a parameter that influences the system's design. The capital cost of the PV rack for retrofitted fences is far lower than all conventional techniques. In addition, the LCOE of the vertical fencing solar agrivoltaic system can be competitive with conventional ground-mounted solar PV for the niche of small-farmers, but further studies are needed for an in-depth cost comparison analysis of the two systems for agrivoltaics and vertical PV fencing systems for large scale applications.

Acknowledgements

This study was supported by the Thompson Endowment.

References

[1] K. S. Hayibo, P. Mayville, R. K. Kailey, and J. M. Pearce, "Water Conservation Potential of Self-Funded Foam-Based Flexible Surface-Mounted Floatovoltaics," *Energies*, vol. 13, no. 23, Art. no. 23, Jan. 2020, doi: 10.3390/en13236285.

[2] SEIA, "Siting, Permitting & Land Use for Utility-Scale Solar," *SEIA*, Nov. 13, 2020. https://www.seia.org/initiatives/siting-permitting-land-use-utility-scale-solar (accessed Nov. 13, 2020).

[3] K. Calvert, J. M. Pearce, and W. E. Mabee, "Toward renewable energy geo-information infrastructures: Applications of GIScience and remote sensing that build institutional capacity," *Renewable and Sustainable Energy Reviews*, vol. 18, pp. 416–429, Feb. 2013, doi: 10.1016/j.rser.2012.10.024.

[4] F. Poggi, A. Firmino, and M. Amado, "Planning renewable energy in rural areas: Impacts on occupation and land use," *Energy*, vol. 155, pp. 630–640, Jul. 2018, doi: 10.1016/j.energy.2018.05.009.

[5] L. Dias, J. P. Gouveia, P. Lourenço, and J. Seixas, "Interplay between the potential of photovoltaic systems and agricultural land use," *Land Use Policy*, vol. 81, pp. 725–735, Feb. 2019, doi: 10.1016/j.landusepol.2018.11.036.

[6] C. de Castro, M. Mediavilla, L. J. Miguel, and F. Frechoso, "Global solar electric potential: A review of their technical and sustainable limits," *Renewable and Sustainable Energy Reviews*, vol. 28, pp. 824–835, Dec. 2013, doi: 10.1016/j.rser.2013.08.040.

[7] P. Engelke, *Foreign policy for an urban world: Global governance and the rise of cities*. Washington, D.C: Atlantic Council, 2015.

[8] P. Denholm and R. M. Margolis, "Land-use requirements and the per-capita solar footprint for photovoltaic generation in the United States," *Energy Policy*, vol. 36, no. 9, pp. 3531–3543, Sep. 2008, doi: 10.1016/j.enpol.2008.05.035.

[9] R. Wüstenhagen, M. Wolsink, and M. J. Bürer, "Social acceptance of renewable energy innovation: An introduction to the concept," *Energy Policy*, vol. 35, no. 5, pp. 2683–2691, May 2007, doi: 10.1016/j.enpol.2006.12.001.

[10] B. Sovacool, "Exploring and Contextualizing Public Opposition to Renewable Electricity in the United States," *Sustainability*, vol. 1, no. 3, pp. 702–721, Sep. 2009, doi: 10.3390/su1030702.

[11] B. K. Sovacool and P. Lakshmi Ratan, "Conceptualizing the acceptance of wind and solar electricity," *Renewable and Sustainable Energy Reviews*, vol. 16, no. 7, pp. 5268–5279, Sep. 2012, doi: 10.1016/j.rser.2012.04.048.

[12] S. Batel, P. Devine-Wright, and T. Tangeland, "Social acceptance of low carbon energy and associated infrastructures: A critical discussion," *Energy Policy*, vol. 58, pp. 1–5, Jul. 2013, doi: 10.1016/j.enpol.2013.03.018.

[13] K. Calvert and W. Mabee, "More solar farms or more bioenergy crops? Mapping and assessing potential land-use conflicts among renewable energy technologies in eastern Ontario, Canada," *Applied Geography*, vol. 56, pp. 209–221, Jan. 2015, doi: 10.1016/j.apgeog.2014.11.028.

[14] S. Nonhebel, "Renewable energy and food supply: will there be enough land?," *Renewable and Sustainable Energy Reviews*, vol. 9, no. 2, pp. 191–201, Apr. 2005, doi: 10.1016/j.rser.2004.02.003.

[15] Nations Unies, Ed., *The world population situation in 2014: a concise report*, illustrated ed. New York: United Nations, 2014.
[16] FAO, "How to Feed the World in 2050." FAO, 2009. Accessed: Oct. 16, 2021. [Online]. Available: http://www.fao.org/fileadmin/templates/wsfs/docs/Issues_papers/HLEF2050_Global_Agriculture.pdf
[17] C. F. Runge and B. Senauer, "How Biofuels Could Starve the Poor," Jan. 28, 2009. Accessed: Oct. 16, 2021. [Online]. Available: https://www.foreignaffairs.com/articles/2007-05-01/how-biofuels-could-starve-poor
[18] J. Tomei and R. Helliwell, "Food versus fuel? Going beyond biofuels," *Land Use Policy*, vol. 56, pp. 320–326, Nov. 2016, doi: 10.1016/j.landusepol.2015.11.015.
[19] P. Thompson, "The Agricultural Ethics of Biofuels: The Food vs. Fuel Debate," *Agriculture*, vol. 2, no. 4, pp. 339–358, Nov. 2012, doi: 10.3390/agriculture2040339.
[20] D. J. Tenenbaum, "Food vs. Fuel: Diversion of Crops Could Cause More Hunger," *Environmental Health Perspectives*, vol. 116, no. 6, Jun. 2008, doi: 10.1289/ehp.116-a254.
[21] C. Dupraz, H. Marrou, G. Talbot, L. Dufour, A. Nogier, and Y. Ferard, "Combining solar photovoltaic panels and food crops for optimising land use: Towards new agrivoltaic schemes," *Renewable Energy*, vol. 36, no. 10, pp. 2725–2732, Oct. 2011, doi: 10.1016/j.renene.2011.03.005.
[22] H. Dinesh and J. M. Pearce, "The potential of agrivoltaic systems," *Renewable and Sustainable Energy Reviews*, vol. 54, pp. 299–308, Feb. 2016, doi: 10.1016/j.rser.2015.10.024.
[23] D. D. Mavani, P. M. Chauhan, and V. P. Joshi, "Beauty of Agrivoltaic System regarding double utilization of same piece of land for Generation of Electricity & Food Production," *International Journal of Scientific & Engineering Research V*, vol. 10, no. 6, 2019.
[24] B. Mow, "Solar Sheep and Voltaic Veggies: Uniting Solar Power and Agriculture," *State, Local, & Tribal Governments*, Jun. 2018. https://www.nrel.gov/state-local-tribal/blog/posts/solar-sheep-and-voltaic-veggies-uniting-solar-power-and-agriculture.html (accessed Oct. 18, 2021).
[25] E. H. Adeh, S. P. Good, M. Calaf, and C. W. Higgins, "Solar PV Power Potential is Greatest Over Croplands," *Sci Rep*, vol. 9, no. 1, p. 11442, Dec. 2019, doi: 10.1038/s41598-019-47803-3.
[26] S. Ravi *et al.*, "Colocation opportunities for large solar infrastructures and agriculture in drylands," *Applied Energy*, vol. 165, pp. 383–392, Mar. 2016, doi: 10.1016/j.apenergy.2015.12.078.
[27] A. M. Pringle, R. M. Handler, and J. M. Pearce, "Aquavoltaics: Synergies for dual use of water area for solar photovoltaic electricity generation and aquaculture," *Renewable and Sustainable Energy Reviews*, vol. 80, pp. 572–584, Dec. 2017, doi: 10.1016/j.rser.2017.05.191.
[28] H. Marrou, J. Wery, L. Dufour, and C. Dupraz, "Productivity and radiation use efficiency of lettuces grown in the partial shade of photovoltaic panels," *European Journal of Agronomy*, vol. 44, pp. 54–66, Jan. 2013, doi: 10.1016/j.eja.2012.08.003.
[29] Y. Elamri, B. Cheviron, J.-M. Lopez, C. Dejean, and G. Belaud, "Water budget and crop modelling for agrivoltaic systems: Application to irrigated lettuces," *Agricultural Water Management*, vol. 208, pp. 440–453, Sep. 2018, doi: 10.1016/j.agwat.2018.07.001.
[30] P. R. Malu, U. S. Sharma, and J. M. Pearce, "Agrivoltaic potential on grape farms in India," *Sustainable Energy Technologies and Assessments*, vol. 23, pp. 104–110, Oct. 2017, doi: 10.1016/j.seta.2017.08.004.
[31] S. Amaducci, X. Yin, and M. Colauzzi, "Agrivoltaic systems to optimise land use for electric energy production," *Applied Energy*, vol. 220, pp. 545–561, Jun. 2018, doi: 10.1016/j.apenergy.2018.03.081.
[32] T. Sekiyama and A. Nagashima, "Solar Sharing for Both Food and Clean Energy Production: Performance of Agrivoltaic Systems for Corn, A Typical Shade-Intolerant Crop," *Environments*, vol. 6, no. 6, p. 65, Jun. 2019, doi: 10.3390/environments6060065.
[33] H. Marrou, L. Guilioni, L. Dufour, C. Dupraz, and J. Wery, "Microclimate under agrivoltaic systems: Is crop growth rate affected in the partial shade of solar panels?," *Agricultural and Forest Meteorology*, vol. 177, pp. 117–132, Aug. 2013, doi: 10.1016/j.agrformet.2013.04.012.

[34] M. H. Riaz, H. Imran, H. Alam, M. A. Alam, and N. Z. Butt, "Crop-specific Optimization of Bifacial PV Arrays for Agrivoltaic Food-Energy Production: The Light-Productivity-Factor Approach," *arXiv:2104.00560 [physics]*, Apr. 2021, Accessed: Oct. 18, 2021. [Online]. Available: http://arxiv.org/abs/2104.00560
[35] P. Santra, P. C. Pande`, S. Kumar`, D. Mishra, and R. Singh, "Agri-voltaics or Solar farming: the concept of integrating solar PV based electricity generation and crop production in a single land use system," *International Journal of Renewable Energy Research (IJRER)*, vol. 7, no. 2, Art. no. 2, Jun. 2017.
[36] T. F. Guerin, "Impacts and opportunities from large-scale solar photovoltaic (PV) electricity generation on agricultural production," *Environmental Quality Management*, vol. 28, no. 4, pp. 7–14, 2019, doi: 10.1002/tqem.21629.
[37] G. A. Barron-Gafford *et al.*, "Agrivoltaics provide mutual benefits across the food–energy–water nexus in drylands," *Nat Sustain*, vol. 2, no. 9, pp. 848–855, Sep. 2019, doi: 10.1038/s41893-019-0364-5.
[38] A. S. Pascaris, C. Schelly, and J. M. Pearce, "A First Investigation of Agriculture Sector Perspectives on the Opportunities and Barriers for Agrivoltaics," *Agronomy*, vol. 10, no. 12, Art. no. 12, Dec. 2020, doi: 10.3390/agronomy10121885.
[39] A. S. Pascaris, C. Schelly, L. Burnham, and J. M. Pearce, "Integrating solar energy with agriculture: Industry perspectives on the market, community, and socio-political dimensions of agrivoltaics," *Energy Research & Social Science*, vol. 75, p. 102023, May 2021, doi: 10.1016/j.erss.2021.102023.
[40] A. S. Pascaris, C. Schelly, M. Rouleau, and J. M. Pearce, "Do Agrivoltaics Improve Public Support for Solar Photovoltaic Development? Survey Says: Yes!," SocArXiv, preprint, May 2021. doi: 10.31235/osf.io/efasx.
[41] D. Feldman, V. Ramasamy, R. Fu, A. Ramdas, J. Desai, and R. Margolis, "U.S. Solar Photovoltaic System and Energy Storage Cost Benchmark: Q1 2020," National Renewable Energy Laboratory, Golden, CO, USA, Technical Report NREL/TP-6A20-77324, Jan. 2021. Accessed: Oct. 01, 2021. [Online]. Available: https://www.nrel.gov/news/program/2021/documenting-a-decade-of-cost-declines-for-pv-systems.html
[42] S. Masna, S. M. Morse, K. S. Hayibo, and J. M. Pearce, "The Potential for Fencing to be Used as Low-Cost Solar Photovoltaic Racking (To be published),", Nov. 10, 2021.
[43] P. R. Bird, "Tree windbreaks and shelter benefits to pasture in temperate grazing systems," *Agroforestry Systems*, vol. 41, no. 1, pp. 35–54, Apr. 1998, doi: 10.1023/A:1006092104201.
[44] H. A. Cleugh, "Effects of windbreaks on airflow, microclimates and crop yields," *Agroforestry Systems*, vol. 41, no. 1, pp. 55–84, Apr. 1998, doi: 10.1023/A:1006019805109.
[45] Matej Vidrih and Stanislav Trdan, "Evaluation of different designs of temporary electric fence systems for the protection of maize against wild boar (Sus scrofa L., Mammalia, Suidae)," *Acta agriculturae Slovenica*, vol. 91, no. 2, pp. 343–349, Nov. 2008, doi: 10.2478/v10014-008-0014-5.
[46] K. VerCauteren, M. Lavelle, and S. Hygnstrom, "A Simulation Model for Determining Cost-Effectiveness of Fences for Reducing Deer Damage," *USDA Wildlife Services - Staff Publications 106*, p. 8, Aug. 2006.
[47] "Standard Fencing Measures - LSB." https://www.lifestyleblock.co.nz/lifestyle-file/running-the-farm/fencing/item/937-standard-fencing-measures (accessed Oct. 12, 2021).
[48] "CIR851/AE017: Construction of High Tensile Wire Fences." https://edis.ifas.ufl.edu/publication/AE017 (accessed Oct. 12, 2021).
[49] F. and F. Ministry of Agriculture, "B.C. Agricultural Fencing Handbook - Province of British Columbia." https://www2.gov.bc.ca/gov/content/industry/agriculture-seafood/business-market-development/structures-mechanization/agricultural-structures-fencing (accessed Oct. 12, 2021).
[50] J. M. Freeman *et al.*, "System Advisor Model (SAM) General Description (Version 2017.9.5)," Technical Report NREL/TP--6A20-70414, 1440404, May 2018. doi: 10.2172/1440404.

[51] M. P. Nair and K. Nithiyananthan, “An Effective Cable Sizing Procedure Model for Industries and Commerial Buildings,” *IJECE*, vol. 6, no. 1, pp. 34–39, Feb. 2016, doi: 10.11591/ijece.v6i1.8391.
[52] L.-P. Hayoun and A. Arrigoni, *Les installations photovoltaïques: conception et dimensionnement des installations raccordées au réseau*, Eyrolles. Paris: Eyrolles, 2012. Accessed: Oct. 15, 2021. [Online]. Available: http://search.ebscohost.com/login.aspx?direct=true&scope=site&db=nlebk&db=nlabk&AN=594416
[53] H. Joshi, “Cables,” in *Residential, Commercial and Industrial Electrical Systems*, vol. 1, 2 vols., McGraw-Hill Education, 2008. Accessed: Oct. 12, 2021. [Online]. Available: https://www.accessengineeringlibrary.com/content/book/9780070620964/chapter/chapter12
[54] Enphase Store, “Enphase IQ 7 Microinverter,” *Enphase Store IQ7 Microinverter*, Oct. 01, 2021. https://store.enphase.com/storefront/en-us/iq7-microinverter-2 (accessed Oct. 01, 2021).
[55] J. Yuan, F. Blaabjerg, Y. Yang, A. Sangwongwanich, and Y. Shen, “An Overview of Photovoltaic Microinverters: Topology, Efficiency, and Reliability,” in *2019 IEEE 13th International Conference on Compatibility, Power Electronics and Power Engineering (CPE-POWERENG)*, Apr. 2019, pp. 1–6. doi: 10.1109/CPE.2019.8862334.
[56] R. Hasan, S. Mekhilef, M. Seyedmahmoudian, and B. Horan, “Grid-connected isolated PV microinverters: A review,” *Renewable and Sustainable Energy Reviews*, vol. 67, pp. 1065–1080, Jan. 2017, doi: 10.1016/j.rser.2016.09.082.
[57] Trina Solar, “Trina Solar TSM-230 Specsheet.” Trina Solar, Sep. 2018. Accessed: Oct. 13, 2021. [Online]. Available: https://static.trinasolar.com/sites/default/files/PC05_Datasheet_40mm_EN.pdf
[58] K. S. Hayibo, “Optimal inverter and wire selection for solar photovoltaic small-scale fencing applications,” *OSF*, 2021, doi: 10.17605/OSF.IO/HJU4D.
[59] NREL, “LK Script - System Advisor Model (SAM),” *NREL System Advisor Model*, Oct. 13, 2021. https://sam.nrel.gov/lk-script.html (accessed Oct. 13, 2021).
[60] K. S. Hayibo and J. M. Pearce, “A review of the value of solar methodology with a case study of the U.S. VOS,” *Renewable and Sustainable Energy Reviews*, vol. 137, p. 110599, Mar. 2021, doi: 10.1016/j.rser.2020.110599.
[61] A. Phinikarides, N. Kindyni, G. Makrides, and G. E. Georghiou, “Review of photovoltaic degradation rate methodologies,” *Renewable and Sustainable Energy Reviews*, vol. 40, pp. 143–152, Dec. 2014, doi: 10.1016/j.rser.2014.07.155.
[62] P. Gilman, “SAM Photovoltaic Model Technical Reference,” National Renewable Energy Lab. (NREL), Golden, CO (United States), Golden, CO, USA, Technical Report NREL/TP-6A20-64102, May 2015. doi: 10.2172/1215213.
[63] M. Woodhouse *et al.*, “On the Path to SunShot. The Role of Advancements in Solar Photovoltaic Efficiency, Reliability, and Costs,” National Renewable Energy Laboratory, Golden, CO, USA, Technical Report NREL/TP--6A20-65872, 1253983, May 2016. doi: 10.2172/1253983.
[64] A. Sangwongwanich, Y. Yang, D. Sera, and F. Blaabjerg, “Lifetime Evaluation of Grid-Connected PV Inverters Considering Panel Degradation Rates and Installation Sites,” *IEEE Transactions on Power Electronics*, vol. 33, no. 2, pp. 1225–1236, Feb. 2018, doi: 10.1109/TPEL.2017.2678169.
[65] K. Branker, M. J. M. Pathak, and J. M. Pearce, “A review of solar photovoltaic levelized cost of electricity,” *Renewable and Sustainable Energy Reviews*, vol. 15, no. 9, pp. 4470–4482, Dec. 2011, doi: 10.1016/j.rser.2011.07.104.
[66] C. S. Lai and M. D. McCulloch, “Levelized cost of electricity for solar photovoltaic and electrical energy storage,” *Applied Energy*, vol. 190, pp. 191–203, Mar. 2017, doi: 10.1016/j.apenergy.2016.12.153.
[67] M. H. Kang and A. Rohatgi, “Quantitative analysis of the levelized cost of electricity of commercial scale photovoltaics systems in the US,” *Solar Energy Materials and Solar Cells*, vol. 154, pp. 71–77, Sep. 2016, doi: 10.1016/j.solmat.2016.04.046.

[68] "Products Brochures & Price Lists - Havells India," *Products Brochures & Price Lists*, Sep. 29, 2021. https://www.havells.com/en/experience-zone/brochures-and-price-lists.html#gref (accessed Sep. 29, 2021).
[69] Polycab, "Polycab Wires & Cables Pricelist – Vashi Electricals," *Polycab Price List Download*, Sep. 29, 2021. https://vashielectricals.com/pricelist/polycab-wires-cables/ (accessed Sep. 29, 2021).
[70] Thermal Zero, "Amazon.com: Snap Strip Stainless Steel Zip Tie 10 Pack 14" Long Locking Cable Tie : Electronics," *Cable Ties*, Oct. 25, 2021. https://www.amazon.com/Strip-Stainless-Steel-Locking-Cable/dp/B004C3C22K (accessed Oct. 25, 2021).
[71] A. Gharakhani Siraki and P. Pillay, "Study of optimum tilt angles for solar panels in different latitudes for urban applications," *Solar Energy*, vol. 86, no. 6, pp. 1920–1928, Jun. 2012, doi: 10.1016/j.solener.2012.02.030.
[72] M. Z. Jacobson and V. Jadhav, "World estimates of PV optimal tilt angles and ratios of sunlight incident upon tilted and tracked PV panels relative to horizontal panels," *Solar Energy*, vol. 169, pp. 55–66, Jul. 2018, doi: 10.1016/j.solener.2018.04.030.
[73] J. A. Duffie and W. A. Beckman, "Chapter 1: Solar Radiation," in *Solar Engineering of Thermal Processes*, 4th ed., Hoboken, New Jersey, USA: John Wiley & Sons, Inc., 2013. Accessed: Nov. 10, 2021. [Online]. Available: https://nbn-resolving.org/urn:nbn:de:101:1-201411102948
[74] D. M. Kadam, A. R. Dange, and V. P. Khambalkar, "Performance of solar power fencing system for agriculture.," *International Journal of Agricultural Technology*, vol. 7, no. 5, pp. 1199–1209, 2011.
[75] G. Nair, M. Chawla, and N. Bawane, "Automatic Farming for Minimum Water Usage and Animal Protection Using Solar Fencing with GSM," in *2020 International Conference on Innovative Trends in Information Technology (ICITIIT)*, Feb. 2020, pp. 1–6. doi: 10.1109/ICITIIT49094.2020.9071530.
[76] K. D. Sharma, S. S. S. Sharma, P. Sharma, and A. Saxena, "Solar Based Electric Fence for Smart Farming," *International Journal of Electrical Power System and Technology*, vol. 2, no. 1, Art. no. 1, Jan. 2016, doi: 10.37628/ijepst.v2i1.229.
[77] A. V. Wakode, S. K. Dindorkar, P. B. Kale, and V. N. Madansure, "Solar electric fencing on farm in Vidarbha region of Maharastra, India.," *International Journal of Agricultural Engineering*, vol. 1, no. 2, pp. 140–143, 2008.
[78] S. K. Lowder, J. Skoet, and T. Raney, "The Number, Size, and Distribution of Farms, Smallholder Farms, and Family Farms Worldwide," *World Development*, vol. 87, pp. 16–29, Nov. 2016, doi: 10.1016/j.worlddev.2015.10.041.
[79] H. Ritchie, "Smallholders produce one-third of the world's food, less than half of what many headlines claim," *Our World in Data*, Aug. 06, 2021. https://ourworldindata.org/smallholder-food-production (accessed Nov. 01, 2021).
[80] L. Grafman and J. Pearce, *To catch the sun*. California, USA: Humboldt State University Press, 2021.
[81] C. G. Bates, "The windbreak as a farm asset.," *undefined*, p. 16, 1937.
[82] W. M. Cornelis and D. Gabriels, "Optimal windbreak design for wind-erosion control," *Journal of Arid Environments*, vol. 61, no. 2, pp. 315–332, Apr. 2005, doi: 10.1016/j.jaridenv.2004.10.005.
[83] J. R. Brandle, B. B. Johnson, and T. Akeson, "Field Windbreaks: Are They Economical?," *Journal of Production Agriculture*, vol. 5, no. 3, pp. 393–398, Jul. 1992, doi: 10.2134/jpa1992.0393.
[84] L. Hodges and J. Brandle, "Windbreaks: An Important Component in a Plasticulture System," *Agronomy & Horticulture -- Faculty Publications*, Jul. 1996, [Online]. Available: https://digitalcommons.unl.edu/agronomyfacpub/391
[85] J. R. Brandle, L. Hodges, and X. H. Zhou, "Windbreaks in North American agricultural systems," *Agroforestry Systems*, vol. 61, no. 1, pp. 65–78, Jul. 2004, doi: 10.1023/B:AGFO.0000028990.31801.62.
[86] M. Wiesmeier, M. Lungu, V. Cerbari, B. Boincean, R. Hübner, and I. Kögel-Knabner, "Rebuilding soil carbon in degraded steppe soils of Eastern Europe: The importance of windbreaks and improved

cropland management," *Land Degradation & Development*, vol. 29, no. 4, pp. 875–883, 2018, doi: 10.1002/ldr.2902.
[87] M. Ito, K. Kato, K. Komoto, T. Kichimi, and K. Kurokawa, "A comparative study on cost and life-cycle analysis for 100 MW very large-scale PV (VLS-PV) systems in deserts using m-Si, a-Si, CdTe, and CIS modules," *Progress in Photovoltaics: Research and Applications*, vol. 16, no. 1, pp. 17–30, 2008, doi: 10.1002/pip.770.
[88] M. Ito, S. Lespinats, J. Merten, P. Malbranche, and K. Kurokawa, "Life cycle assessment and cost analysis of very large-scale PV systems and suitable locations in the world," *Progress in Photovoltaics: Research and Applications*, vol. 24, no. 2, pp. 159–174, 2016, doi: 10.1002/pip.2650.
[89] H. Ritchie and M. Roser, "Energy," *Our World in Data*, Nov. 28, 2020. https://ourworldindata.org/energy-access (accessed Nov. 01, 2021).